

Biofabrication of Zinc oxide nanoparticles and their *in-vitro* cytotoxicity towards gastric cancer (MGC803) cell lines.

Chongyao Bi^{1#}, Jianwei Li^{2#}, Lijun Peng³, Jianmin Zhang^{4*}

¹Department of General Surgery, Jiao Zhou Central Hospital of Qing Dao, Qing Dao City, Shan Dong Province, PR China

²Department of General surgery, People's Hospital of Linshu County, Shan Dong Province, PR China

³Department of Gastroenterology, Linyi People's Hospital, Lin Yi City, Shan Dong Province, PR China

⁴Department of General Surgery, Linyi People's Hospital, Lin Yi City, Shan Dong Province, PR China

#These two authors contribute to this study equally

Abstract

This present report describes the green approach for the preparation of zinc oxide nanoparticles (ZnO NPs) using *Murraya keenigii* leaf extract by an eco-friendly approach. The produced ZnO NPs were characterized by using techniques such as X-Ray Diffraction (XRD), Fourier Transform Infrared (FTIR), Ultra Violet-Visible (UV-Vis), Energy Dispersive Spectroscopy (EDS) and Transmission Electron Microscopy (TEM). TEM and Dynamic Light Scattering (DLS) results have confirmed the formation of spherical ZnO NPs with average size of 20 nm. Further, the cytotoxicity results of the synthesized ZnO NPs showed their excellent biocompatibility towards gastric cancer (MGC803) cell lines, extending their scope of applications in biomedicine.

Keywords: ZnO NPs, *Murraya keenigii* leaf, Cytotoxicity, Gastric cancer.

Accepted on October 6, 2016

Introduction

Zinc Oxide Nanoparticles (ZnO NPs) are unique class of materials that shows properties such as piezoelectric, semiconducting, pyro electric and exhibiting applications in piezoelectric devices, electronics, chemical sensors, coatings, cosmetics, paints, spin electronics and UV light emitters [1-3]. ZnO NPs also have applications in industries producing photo catalysts, gas sensors, solar cells, UV light emitting devices, pharmaceutical and cosmetics [4-8]. ZnO NPs can be synthesized by various methods such as spray pyrolysis [9], precipitation [10,11], thermal decomposition [12], sol-gel synthesis [13], hydrothermal synthesis [14-17], photochemical reduction and electrochemical methods [18,19]. Because of increase in demand for eco-friendly approaches has led to the development of new biosynthetic methods for the preparation of ZnO NPs.

Natural plant extracts and their bioconstituents offer biosynthetic approaches for different metal and metal oxide nanoparticles which environment friendly are allowing a controlled synthesis with tuneable shape and size [20]. It is well known that the biomolecules present in the plant extract play role in the synthesis of nanoparticles. The bacteria [21] and enzymes [22] have already been used for the eco-friendly preparation of ZnO NPs.

In recent days, various metal and metal oxide nanoparticles are having high demand in market due to their good photostability, non-toxicity, high fluorescence, solubility and excellent biocompatibility. For instance, Lin et al., have reported the excellent biocompatibility of AuNPs against gastric cancer cell lines [23]. Hence, there is an increasing demand for the development of new biocompatible metal and metal oxide nanoparticles for future cancer therapy applications.

In the present work, we used the leaf extract of *Murraya keenigii* plant for the eco-friendly synthesis of ZnO NPs. The polyphenols that are present in the extract of *Murraya keenigii* plant play key role in the reduction and stabilization process. Further the prepared ZnO NPs are studied for their cytotoxicity towards the gastric cancer (MGC803) cell lines.

Materials and Methods

Materials

All the chemicals and reagents used in the experiments were purchased from Sigma-Aldrich Ltd, Shanghai. All the glass vessels used were initially cleaned with acid solution and double distilled water. Double distilled water was used for preparation of ZnO NPs.

Preparation of ZnO NPs

3 g of dried *Murraya keenigii* leaves were weighed and ground well using a mortar pestle and added to 20 mL of double distilled water. The mixture was then heated at 90°C for about 1 h and filtered using cellulose nitrate filter paper to obtain an extract solution. ZnO NPs were prepared by the reduction of ZnNO₃ using leaf extract, containing bioconstituents which acts as stabilizing agent.

About 20 mL of prepared *Murraya keenigii* leaf extract was added 60 mL 0.01 M ZnNO₃ precursor solution and the resulting solution was heated at 100°C for 30 min to obtain a yellow precipitate which later was washed twice with ethanol. The obtained product was then annealing at 300°C for 1 h to get white powder of ZnO NPs.

Cytotoxicity evaluation

To check the potentiality of ZnO NPs for biomedical applications, we have checked the cytotoxicity of prepared NPs towards gastric cancer cell lines. The cytotoxicity assay on MGC803 cancer cells was conducted by following 3-[4,5-dimethylthiazol-2-yl]-2,5-diphenyltetrazolium bromide (MTT) assay. A cell density of about 1×10^4 cells per well was seeded in a 96-well plate and followed by incubation for about 24 h. After the incubation period, the media was discarded and a fresh media was added along with following incubation at 37°C for 24 h. Then, the media was discarded and washed two times with Phosphate Buffer Solution (PBS). An MTT reagent (5 mg/mL) was added to all the wells and incubated for 4 hours. Later, medium containing unreduced MTT was discarded and 100 μ L of DimethylSulfoxide (DMSO) was added to dissolve the MTT reagent. On the other hand, a control experiment was performed without the addition of ZnO NPs. The optical absorbance of each well was then recorded at 570 nm using a microplate reader.

Characterization

The optical properties of prepared ZnO NPs were analysed by UV-visible absorption spectra. UV-Visible (Shimadzu) instrument was used for measurements. Perkin-Elmer X-ray diffraction instrument was used for X-Ray Diffraction (XRD) characterizations. Measurements were carried out in the range from 20° to 80° Cu K α radiations ($k = 1/4$, 0.15406 nm). Morphology and shape of ZnO NPs were characterized by JEM 2100 (JEOL, Tokyo, Japan) transmission Electron Microscopy instrument. Additionally, Energy dispersive spectroscopy analysis for ZnO NPs was studied by using RONTEC'S EDX system. JASCO, Tokyo, Japan, Fourier Transform Infrared (FTIR) instrument was used for FTIR analysis to know about surface capping. Samples for FTIR studies were prepared by mixing dried product with KBr powder and pelletized. Further, the zeta potential and size distribution of the ZnO NPs were analyzed by using a SZ-100; Horiba Scientific nanoparticles analyser (Edison, NJ, USA). About, 1 mL of prepared ZnO colloid was diluted four times with milli pore water and measured under the instrument.

Results

The XRD pattern of biofabricated ZnO NPs using leaf extract of *Murraya keenigii* is represented in Figure 1. The XRD pattern showed the diffraction peaks at 32.1°, 34.23°, 36.21°, 47.34°, 56.44°, 62.78°, 67.78°, 68.89°, and 76.79° characteristic to indexing planes (100), (002), (101), (102), (110), (103), (112), (201) and (202) correspondingly, signifying the hexagonal structure of the NPs (JCPDS card No.89-7102).

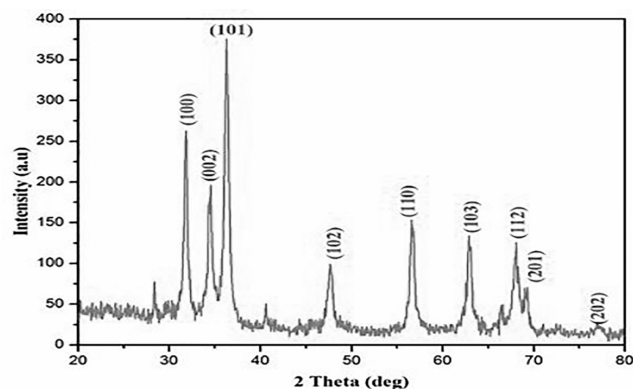


Figure 1. X-ray diffraction patterns of ZnO NPs.

Figure 2 represented the TEM images and Selected Area Electron Diffraction (SAED) pattern for the biofabricated ZnO NPs. It is found that the NPs are hexagonal with a mean particle size of 20 nm (also confirmed from DLS data). The SAED pattern revealed that the synthesized ZnO NPs were crystalline and polydispersed in nature (Shown in Figure 2B).

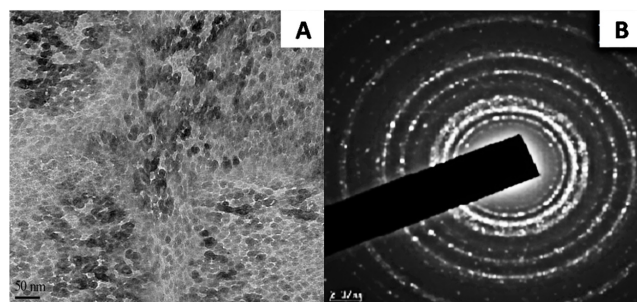


Figure 2. A) TEM image; B) SAED pattern of biosynthesized ZnO NPs.

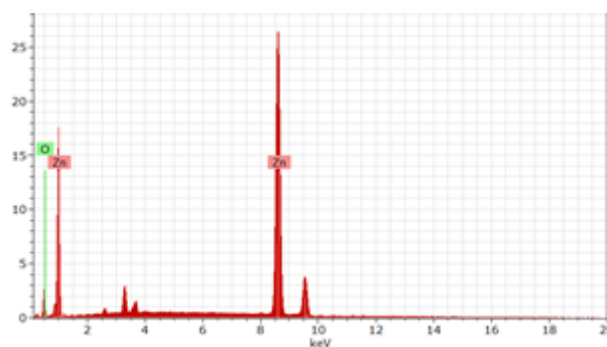


Figure 3. Energy-dispersive X-ray spectroscopy spectrum of prepared ZnO NPs.

Figure 3 represented the Energy-Dispersive X-ray Spectroscopy (EDS) for the prepared ZnO NPs, which shows the existence of peaks related to oxygen and zinc confirming the ZnO NPs. On the other hand, Figure 4 represented the FTIR spectrum of the plant extract mediated ZnO NPs. The presence of peak at 510 cm^{-1} , corresponding to the Zn-O bond stretching vibrations [24] the bands shown at 1088 cm^{-1} and $3,420\text{ cm}^{-1}$ are characteristic to the stretching vibrations of symmetric C-O and O-H groups [25]. The vibrational bands at $1,643\text{ cm}^{-1}$, 2916 cm^{-1} signifies the stretching of C=O and C-H functionalities respectively.

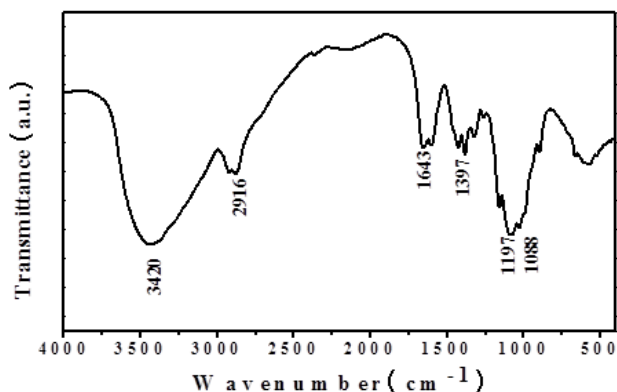


Figure 4. Fourier transform-infrared spectroscopy spectrum of prepared ZnO NPs.

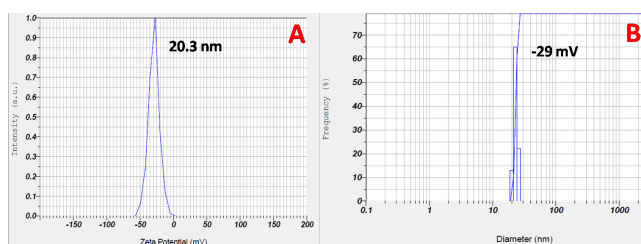


Figure 5. A) Dynamic light scattering; B) zeta potential of ZnO NPs.

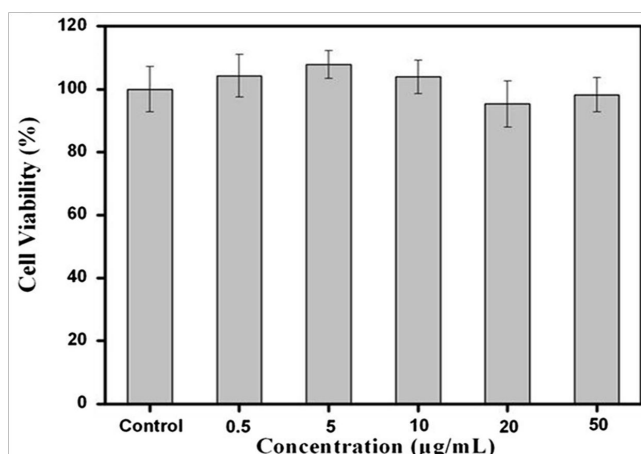


Figure 6. Cell viability of MGC803 cells induced by ZnO NPs.

The zeta potential and size distribution of the ZnO NPs are represented in Figure 5. From the DLS data, the mean particle size is found to be 20 nm and most of the particles lied in the

range from 10 to 30 nm (also evidenced from TEM results). On the other hand, surface charge of the prepared nanoparticles is -29 mV.

An MTT assay was performed to know the cell viability of MGC803 cancer cells treated with various concentrations of ZnO NPs. From Figure 6, it is found that a very negligible cell death of MGC803 cells is observed even after their treatment with the highest concentration (50 µg/mL) of ZnO NPs. From the figure, it is also revealed that, no significant cytotoxicity of ZnO NPs in the concentration range of 0-50 µg/mL. On the other hand, the cell viability is found to be more than 95% when compared with control group.

Discussion

The structural properties and crystalline size of the synthesized ZnO NPs are known by powder X-ray diffraction analysis. All the diffraction peaks in the XRD pattern (Shown in Figure 1) confirmed the wurtzite structure of hexagonal ZnO NPs [11,26]. On the other hand, the narrow and sharp well defined diffraction peaks signify that the prepared ZnO NPs are well crystalline in nature. The average crystalline size (D) of the synthesized ZnO NPs was calculated from Scherrer equation, $D=0.89 \lambda /(\beta \cos \theta)$.

Where β is full width half-maximum, λ is the wavelength of (101) plane line of the ZnO NPs and θ is the diffraction angle. The measured average crystallite size of the ZnO NPs is 18 nm. The formation of ZnO NP is confirmed by naked eye with the change of the colour of reaction solution during synthesis. The reaction of leaf extract of *Murraya keenigii* with ZnNO₃ resulted in colour change with the formation of yellow colour precipitate within 30 min. It is found that the present synthesis is faster than the previous reports on green synthesis of ZnO NPs [27-29]. On the other hand, the blank reaction that is conducted without the addition of plant extract remained same without any change even after 72 h, signifying the role of *Murraya keenigii* extract in the reduction of ZnNO₃.

Further the formation of ZnO NPs by *Murraya keenigii* leaf extract is also confirmed by EDS and TEM results. The EDS spectrum revealed the existence of extra peaks other than zinc and oxygen which may be because of the biomolecules that are adsorbed on the surface of synthesized ZnO NPs without any extra impurity, indicating the purity of the prepared ZnO NPs. Further, the FTIR results revealed the information about the surface capping of ZnO NPs with phytoconstituents of the *Murraya keenigii* plant extract. The presence of vibrational bands corresponding to O-H and C-O functionalities signified the stabilization of ZnO NPs with the secondary metabolites of *Murraya keenigii* plant extract [30,31]. On the other hand, the presence of bands related to ketone functionalities indicating that the hydroxyl groups of polyphenols are involving the reduction which further converting to their ketone forms after reduction. Further, the FTIR results are supported by negative zeta potential of the ZnO NPs. The negative surface charge of the plant extract mediated ZnO NPs may be because of the adsorbed phenolic functional groups of plant extract that

existed on the surface of NPs. These negative surface charges may further generate repulsions among NPs, leading to their stability.

An MTT assay was performed to determine the biocompatibility and potential of the ZnO NPs for biomedical applications. It is well known that various nanoparticles show cytotoxicity towards different cancer cell lines. The cytotoxicity of nanoparticles mainly depends on their shape, size and surface modification. On the other hand, the effect of the size of AuNPs on *in vitro* cytotoxicity in HeLa cells has already been proved. Maddinedi et al., have showed the size dependent cytotoxicity of AuNPs towards A549 and HCT116 cell lines [32]. Indeed, Hauck et al., [33] and Panet et al., [34] have shown that the size of the particle, and not the capping agent, is responsible for determining the toxicity of AuNPs. Moreover, there have been no systematic studies comparatively analysing the size and dose dependent cytotoxic behaviour of AuNPs synthesized using diastase towards two different cell lines.

In the present work, we have studied the cytotoxicity of ZnO NPs against MGC803 cell lines. Figure 6 have showed that the prepared ZnO NPs are non-toxic and exhibited more biocompatibility towards MGC803 cancer cells within 0~50 µg/m. From these results, we can confirm the high biocompatibility of synthesized ZnO NPs, signifying their important role in biological applications.

Conclusions

A low-cost, simple and eco-friendly synthetic approach for the preparation of ZnO NPs using *Murraya keenigii* leaf extract is proposed in this work. Zeta potential and FTIR results revealed the capping of ZnO NPs with *Murraya keenigii* extract polyphenols. HRTEM and DLS data confirmed the spherical ZnO NPs with mean size of 20 nm. The prepared ZnO NPs exhibited excellent biocompatibility towards MGC803 cell lines, extending their scope of applications in biomedicine.

References

1. Wang ZL. Nanostructures of zinc oxide. *Mater Today* 2004; 7: 26-33.
2. Wahab R, Kim YS, Lee DS, Seo JM, Shin HS. Controlled synthesis of zinc oxide nanoneedles and their transformation to microflowers. *Sci Adv Mater* 2010; 2: 35-42.
3. Akhtar MS, Ameen S, Ansari SA, Yang O. Characterization of ZnO nanorods and balls nanomaterials for dye sensitized solar cells. *J Nanoeng Nanomanuf* 2011; 1: 71-76.
4. Deng Z, Chen M, Gu G, Wu LM. A facile method to fabricate ZnO hollow spheres and their photocatalytic property. *J Phys Chem B* 2008; 112: 16-22.
5. Yang SJ, Park CR. Facile preparation of monodisperse ZnO quantum dots with high quality photoluminescence characteristics. *Nanotechnology* 2008; 19: 035609.
6. Krishnakumar T, Jayaprakash R, Pinna N, Singh VN, Mehta BR, Phani AR. Microwave-assisted synthesis and characterization of tin oxide nanoparticles. *Mater Lett* 2008; 63: 242-245.
7. Cao B, Cai W. From ZnO nanorods to nanoplates: chemical bath deposition growth and surface-related emission. *J Phys Chem C* 2008; 112: 680-685.
8. Li M, Bala H, Lv X, Ma X, Sun F, Tang L. Direct synthesis of monodispersed ZnO nanoparticles in an aqueous solution. *Mater Lett* 2007; 61: 690-693.
9. Liu T-Q, Sakurai O, Mizutani N, Kato M. Preparation of spherical fine ZnO particles by the spray pyrolysis method using ultrasonic atomization technique. *J Mater Sci* 1986; 21: 3698-3702.
10. Zhong OP, Matijevic E. Preparation of uniform zinc oxide colloids by controlled double-jet precipitation. *J Mater Chem* 1996; 3: 443-447.
11. Lingna W, Mamoun M. Synthesis of zinc oxide nanoparticles with controlled morphology. *J Mater Chem* 1999; 9: 2871-2878.
12. Andres-Verges M, Martinez-Gallego M. Spherical and rod-like zinc oxide microcrystals: morphological characterization and microstructural evaluation with temperature. *J Mater Sci* 1992; 27: 3756-3762.
13. Bahnemann DW, Kormann C, Hoffmann MR. Preparation and characterization of quantum size zinc oxide: a detailed spectroscopic study. *J Phys Chem* 1987; 91: 3789.
14. Sue K, Murata K, Kimura K, Arai K. Continuous synthesis of zinc oxide nanoparticles in supercritical water. *Green Chem* 2003; 5: 659-662.
15. Sue KW, Kimura K, Yamamoto M, Arai K. Rapid hydrothermal synthesis of ZnO nanorods without organics. *Mater Lett* 2004; 58: 3350-3352.
16. Ohara S, Mousavand T, Umetsu M, Takami S, Adschiri T, Kuroki Y. Hydrothermal synthesis of fine zinc oxide particles under supercritical conditions. *Solid State Ionics* 2004; 172: 261-264.
17. Ohara S, Mousavand T, Sasaki T, Umetsu M, Naka T, Adschiri T. Continuous production of fine zinc oxide nanorods by hydrothermal synthesis in super-critical water. *J Mater Sci* 2008; 43: 2393-2396.
18. Chen W, Cai W, Zhang L, Wang G. Sonochemical processes and formation of gold nanoparticles within pores of mesoporous silica. *J Colloid Interface Sci* 2001; 238: 291-295.
19. Frattini A, Pellegrini N, Nicastro D, Sanctis OD. Effect of amine groups in the synthesis of Ag nanoparticles using aminosilanes. *Mater Chem Phys* 2005; 94: 148-152.
20. Bar H, Bhui DK, Sahoo GP, Sarkar P, Pyne S, Misra A. Green synthesis of silver nanoparticles using seed extract of *Jatropha curcas*. *Colloids Surf A* 2009; 348: 212-216.
21. Jayaseelan C, Abdul Rahuman A, Vishnu Kirthi A, Marimuthu S, Santhoshkumar T, Bagavan A. Novel microbial route to synthesize ZnO nanoparticles using *Aeromonas hydrophila* and their activity against pathogenic bacteria and fungi. *Spectrochim Acta Part A* 2012; 90: 78-84.

22. Prasad K, Jha AK. ZnO nanoparticles: synthesis and adsorption study. *Nat Sci* 2009; 1: 129-135.
23. Lin J, Zhou Z, Li Z, Zhang C, Wang X, Wang K, Gao G, Huang P, Cui D. Biomimetic one-pot synthesis of gold nanoclusters/nanoparticles for targeted tumour cellular dual-modality imaging. *Nanoscale Res Lett* 2013; 170.
24. Rajiv P, Rajeshwari S, Venckatesh R. Bio-fabrication of zinc oxide nanoparticles using leaf extract of *Parthenium hysterophorus* L and its size-dependent antifungal activity against plant fungal pathogens. *Spectrochimica Acta A Mol Biomol Spectrosc* 2013; 112: 384-387.
25. Barros Gomes Camara R, Silva Costa L, Pereira Fidelis G, Duarte Barreto Nobre LT, Dantas-Santos N, Lima Cordeiro S, Santana Santos Pereira Costa M, Guimaraes Alves L, Oliveira Rocha HA. Heterofucans from the brown seaweed *canistrocarpus cervicornis* with anticoagulant and antioxidant activities. *Drugs* 2011; 9: 124-138.
26. Jayaseelan C, Rahuman AA, Kirthi AV, Marimuthu S, Santhoshkumar T, Bagavan A, Gaurav K, Karthik L, Rao KVB. Novel microbial route to synthesize ZnO nanoparticles using *Aeromonas hydrophila* and their activity against pathogenic bacteria and fungi. *Spectrochim Acta A* 2012; 90: 78-84.
27. Abdul Salam H, Sivaraj R, Venckatesh R. Green synthesis and characterization of zinc oxide nanoparticles from *Ocimum basilicum* L var. *purpurascens* Benth-Lamiaceae leaf extract. *Mater Lett* 2014; 131: 16-18.
28. Singh G, Babele PK, Kumar A, Srivastava A, Sinha RP, Tyagi MB. Synthesis of ZnO nanoparticles using the cell extract of the cyanobacterium, *Anabaena* strain L31 and its conjugation with UV-B absorbing compound shinorine. *J Photochem Photobiol Biol* 2014; 138: 55-62.
29. Mohan Kumar K, Badal Kumar M, Kiran Kumar HA, Sireesh Babu M. Green synthesis of size controllable gold nanoparticles. *Spectrochim Acta Mol Biomol Spectrosc* 2013; 116: 539-545.
30. Sireesh Babu M, Badal Kumar M, Raviraj V, Poliraju K, Sreedhara Reddy P. Bioinspired reduced graphene oxide nanosheets using *Terminalia chebula* seeds extract. *Spectrochim Acta Mol Biomol Spectrosc* 2015; 145: 117-124.
31. Hemali P, Pooja M, Sumitra C. Green synthesis of silver nanoparticles from marigold flower and its synergistic antimicrobial potential. *Arab J Chem* 2015; 8: 732-741.
32. Sireesh babu M, Badal Kumar M, Shivendu R, Nandita D. Diastase assisted green synthesis of size controllable gold nanoparticles. *RSC Adv* 2015; 5: 26727-26733.
33. Hauck TS, Ghazani AA, Chan WCW. Assessing the effect of surface chemistry on gold nanorod uptake, toxicity, and gene expression in mammalian cells. *Small* 2008; 4: 153-159.
34. Pan Y, Neuss S, Leifert A, Fischler M, Wen F, Simon U, Schmid G, Brandau W, Jahnhen-Dechent W. Size-dependent cytotoxicity of gold nanoparticles. *Small* 2007; 3: 1941-1949.

***Correspondence to**

Jianmin Zhang
Department of General Surgery
Linyi People's Hospital
Shan Dong Province
PR China